

1 **EFFECTIVENESS ASSESSMENT OF RISK REDUCTION MEASURES AT COASTAL AREAS USING A**
2 **DECISION SUPPORT SYSTEM: FINDINGS FROM EMMA STORM**

3

4 Óscar Ferreira^{1*}, Theocharis A. Plomaritis^{1,2}, Susana Costas¹

5

6 ¹CIMA/FCT, University of Algarve, Campus de Gambelas, 8005-139, Faro, Portugal;

7 oferreir/tplomaritis/scotero@ualg.pt; *corresponding author

8 ²Faculty of Marine and Environmental Science, Department of Earth Science, University of Cadiz,

9 Campus Rio San Pedro (CASEM), Puerto Real 11510, Cadiz, Spain.

10 **Abstract**

11 Storms impact coastal areas often causing damages and losses at occupied areas. On a scenario of
12 increasing human occupation at coastal zones and under climate change conditions (including sea
13 level rise and increasing frequency of extreme sea levels), the consequences of storms are expected
14 to be amplified if no adaptation or further management actions are implemented. The selection of
15 the best possible coastal management measures, considering both costs and effectiveness, will be
16 mandatory in the future, in order to optimise resources. This work analyses the performance of risk
17 reduction measures (beach nourishment and receptors - house and infrastructures - removal), using
18 a decision support system comprised by a morphodynamic numerical model (XBeach) and a Bayesian
19 network based on the source-pathway-receptor concept. The effectiveness of the risk reduction
20 measures is then assessed by a simple index expressing the consequences to the receptors. The
21 approach was tested at Faro Beach by evaluating its performance for a particular storm, Emma
22 (Feb/March 2018), which fiercely impacted the southern coast of Portugal. The output results from
23 the modelling were compared to field observations of the actual damages caused by the storm. The
24 combined use of both measures or the solely use of the nourishment would avoid almost all observed
25 impacts from this storm. The work is pioneer on demonstrating the use of a decision support system

26 for coastal regions validated against observed impacts for a high-energy storm event. The
27 methodology and the proposed index are adaptable to any sandy coastal region and can be used to
28 test (and improve) management options at a broad number of coastal areas worldwide, minimising
29 implementation costs and reducing the risk to the occupation and to the people.

30 Keywords: storm impacts, decision support systems, risk reduction, occupation, management

31 **1. Introduction**

32 Storms affecting sandy coastal areas produce hazards such as erosion, overwash or flooding, which in
33 turn promote risk to life and property damage in occupied areas. These phenomena occur on a global
34 scale, but they have a particular acuity on coasts exposed to high-wave energy and with accentuated
35 human occupation. Historical analysis of storm events and their consequences show that the problems
36 associated with coastal risks are well known and object of study for many decades (see Garnier et al.,
37 2018). The subsequent mitigation measures and management interventions vary according to the type
38 of occupation and the coastal morphology (see Stelljes et al. 2018 for a summary of strategies,
39 measures and results, which can be found at <http://coastal-management.eu>). Despite the historical
40 knowledge of the impact of storms on coastal zones, their occurrence continues to raise problems
41 mostly because of two aspects (Garnier et al., 2018): a "false sense of security" promoted by coastal
42 defence works that protect occupation from small return period events, but may allow the impact of
43 events of greater magnitude; and the loss or lack of "historical memory", corresponding to the
44 frequent forgetfulness of previous situations. In fact, several recent examples show the negative
45 consequences of the impact of low-frequency high-impact events on developed countries along the
46 world: Hurricanes Katrina (2005) and Sandy (2012) in the USA (Link, 2010; Kantha, 2013; Bennington
47 and Farmer, 2015; Clay et al., 2016), storm Xynthia (2010) in France (Bertin et al., 2012), storm
48 Hercules (2014) in the UK (Masselink et al., 2016) or St. Agatha storm (2015) in the Adriatic (Perini et
49 al., 2015). These events raised awareness reminding that even developed coasts and countries can be
50 severely exposed to coastal hazards and face consequences.

51 Furthermore, coastal risk associated with storms is likely to increase in the future due to climate
52 change (e.g. sea level rise and/or changes on storminess) and on-going coastal development (van
53 Dongeren et al., 2018). Extreme sea levels (and associated coastal flooding) are expected to increase
54 their frequency, worldwide, as a consequence of sea level rise (Vitousek et al., 2017; Vousdoukas et
55 al., 2017), increasing the flood risk in the next decades unless timely measures are taken (Vousdoukas
56 et al., 2018a). In the absence of further investments in coastal adaptation, the global expected annual
57 damage is projected to increase by two to three orders of magnitude by the end of the century and
58 the expected annual number of people exposed to coastal flooding to increase by at least one order
59 of magnitude (Vousdoukas et al., 2018b). The latter implies critical preparation and adaptation to
60 minimize future storm impacts (Ciavola et al., 2011a). However, most of the engineering, prevention
61 and mitigation actions are constrained by economics and compromises must be sought between
62 potential consequences and resources available for coastal management (Ciavola et al., 2011b). Thus,
63 coastal authorities will need not only to implement Disaster Risk Reduction (DRR) measures but also
64 to assess their effectiveness on risk prevention using Decision Support Systems – DSS (Ferreira et al.,
65 2018; van Dongeren et al., 2018; van Dongeren et al., 2016; Zanuttigh et al., 2014) in order to be able
66 to opt for the best possible solutions at an optimized cost. This requires extra efforts on the
67 understanding and modelling of the physical forcing, coastal response and consequences towards
68 human occupation.

69 Different approaches to the evaluation of the effectiveness of coastal management plans and actions
70 can be found in several recent works, by using environmental, governance and/or socioeconomic
71 performance indicators (e.g. Wu et al., 2017; Ye et al., 2015), analyses of questionnaires to managers
72 or beach users (e.g. Aretano et al., 2017; López-Rodríguez and Rosado, 2017) or by assessing coastal
73 regulation plans (e.g. Neal et al., 2018). The evaluation of the effectiveness of specific DRR measures
74 by analysing the consequences of their implementation is, however, still limited. The existing works
75 mostly analyse the efficiency and/or the cost-effectiveness of the DRR measures at the scale of years
76 to decades. For example: Burcharth et al. (2014) analysed the upgrading of a typical rock armoured

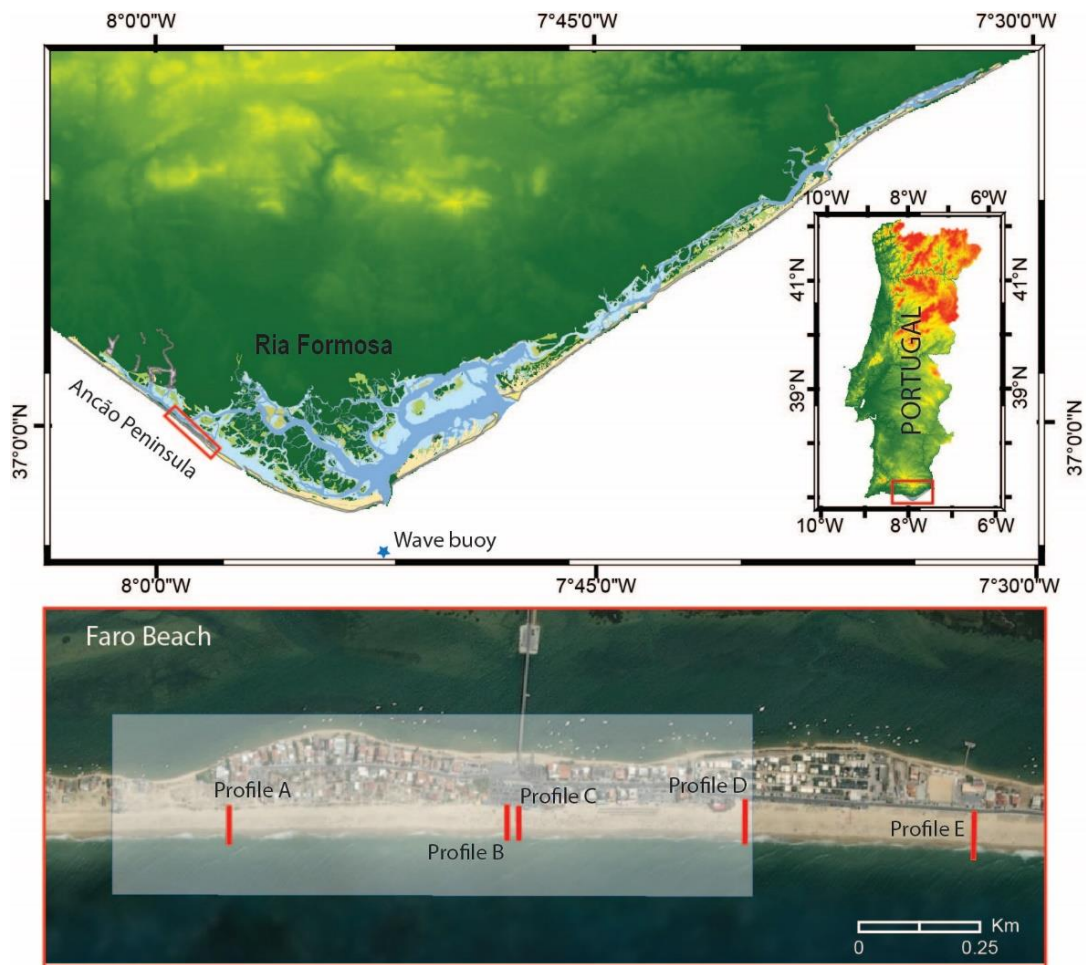
77 revetment to cope with sea level rise predictions for 2100, including a cost optimization analysis;
78 Brown et al. (2016) and Stronkhorst et al. (2018) analysed the cost-effectiveness of different
79 nourishment strategies from short-term (10-20 years) to long-term (up to 100 years); Huguet et al.
80 (2018) evaluated the effectiveness of a managed realignment against existing dikes to prevent floods
81 at La Faute-sur-Mer for 2100. Analysis of the behaviour of specific management interventions (or DRR
82 measures) against the observed impacts of single storms are not yet commonly found in literature,
83 being limited to few recent studies, mostly within the frame of EU funded projects (e.g. Barquet et al.,
84 2018; Bolle et al., 2018; Ferreira et al., 2018; Jäger et al., 2018; Plomaritis et al., 2018; Villatoro et al.,
85 2014). There is not currently in place a policy of ex-ante evaluation of the effectiveness of DRR
86 measures against specific, high potential impact, storm events. In most cases, that evaluation is only
87 made after the event and lessons are learned at the expenses of the observed consequences.
88 Furthermore, only a limited number of works presented the impact of extreme storms in terms of
89 hazards and consequences, and none of them provided (to our knowledge) a full comparison between
90 modelled consequences and observed ones, at the field.

91 This work main goal is to assess the effectiveness of DRR measures against the impact (over houses
92 and infrastructures) of a high-energy event (storm) by using a DSS based on two approaches: a)
93 modelling the impact of a specific storm over a selected area and compare it to the performance of
94 the DRR measures; b) using the basic storm characteristics (wave height and period, and total water
95 level) and a pre-trained Bayesian Network (BN) to estimate the DRR performance. The link between
96 physical drivers and human occupation is fundamental to such assessment, not only on understanding
97 risk levels derived from drivers at a given area, but also on how a better land use and management
98 can contribute to reduce the risk. The DSS used builds upon the works of Poelhekke et al. (2016) and
99 Plomaritis et al. (2018). Effectiveness is here considered as the ability of a given measure to fully
100 prevent consequences (e.g. damage to houses and infrastructures) when compared to the initial
101 situation (comparison of storm impact before and after DRR implementation). The methods were
102 applied to storm Emma (February/March 2018) that highly impacted the Gulf of Cadiz and Faro Beach,

103 southern Portugal, which was selected to test the proposed approaches. The here proposed
104 methodology for DRR effectiveness assessment can be used at any other coastal sandy area prior to
105 the implementation of DRR measures.

106 **2. Study Area**

107 Faro Beach is located at Ancão Peninsula, the westernmost sector of the Ria Formosa barrier island
108 system (Figure 1). This system, triangular in shape and with a total coastline extension of about 55 km,
109 is extremely dynamic. Most of the observed morphological changes are related to inlet dynamics,
110 shoreline evolution, longshore drift, overwash and storm-related processes, dune formation,
111 backbarrier processes and artificial nourishment actions (see Ferreira et al., 2016a). Tides in the area
112 are semi-diurnal, with average ranges of 2.8 m and 1.3 m for spring and neap tides, respectively.
113 Maximum ranges of 3.5 m can be reached during spring equinoctial tides. Wave energy is moderate
114 with an average annual offshore significant wave height of 1.0 m and an average peak period of 8.2 s.
115 Dominant incident waves are from the W–SW (71% of occurrences), although E-SE conditions
116 represent 23% of the total (Costa et al., 2001). The net littoral drift and longshore currents are typically
117 from west to east. Storms are considered as events with significant wave heights (H_s) greater than 2.5
118 m (see Oliveira et al., 2018) or 3 m (see Almeida et al., 2011a, 2011b; Costa et al., 2001), with the SW
119 ones being more energetic, and reaching a H_s of about 8.1 m for a 50 year return period (Pires, 1998).
120 Although no statistically significant linear trends of storm characteristics were identified from the
121 historical reanalysis record (1953 -2001) (Almeida et al., 2011b), storm variability in the area, both in
122 terms of wave height and surge, is correlated with the North Atlantic Oscillation and the East Atlantic
123 Pattern (Plomaritis et al., 2015).



124

125 Figure 1. Location of the case study area, Faro Beach, within the Ria Formosa at the southernmost
 126 coast of Portugal. The lower panel shows an image of the urbanised Faro Beach, including the location
 127 of the pre- and post-storm measured profiles (A to E) while the shaded area highlights the nearshore
 128 area of the model domain.

129 Faro Beach corresponds to the occupied central portion of Ancão Peninsula (see Figure 1) and is
 130 exposed to the W–SW dominant wave conditions. Faro Beach is characterized by a steep beach-face
 131 with an average slope of around 0.1, varying from 0.06 to 0.15 (Vousdoukas et al., 2012a), that can be
 132 classified as ‘reflective’ following Wright and Short (1984). The oceanic beach is generally narrow,
 133 having a beach berm (occasionally a second berm can be observed) with variable width (from less than
 134 15 m to more than 40 m). The width of the peninsula ranges from 50 m to 150 m. A large part of the
 135 dunes within the central part of Faro Beach were lowered and replaced by human occupation such as
 136 infrastructure (car parks and roads) and houses. The shoreline evolution of the Ancão Peninsula for

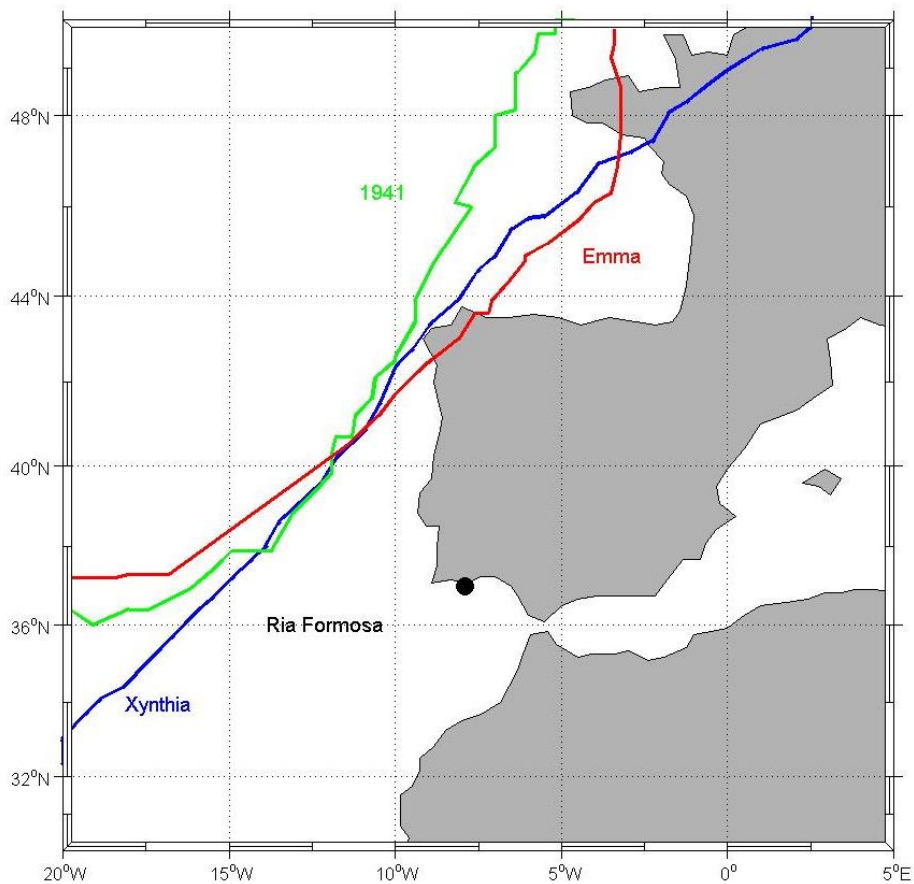
137 the last decades shows a retreat at the western part (up to -0.8 m/year) and accretion to the east
138 (Ferreira et al., 2006; Kombiadou et al., 2018) with the central part of Faro Beach showing some
139 stability. The most relevant coastal hazards at this area have been related to the action of high-energy
140 storms, namely erosion and overwash. In fact, the oceanfront of Faro Beach is often overwashed
141 during spring tides and storms with long period swell waves (Almeida et al., 2012; Rodrigues et al.,
142 2012), causing property damage. Foredune and beach erosion during storms have caused the
143 destruction of houses and roads located at the shorefront (Almeida et al., 2012). Storms with return
144 periods on the order of 25/50 years are expected to promote dune retreat on the order of 15/25 m,
145 respectively (Almeida et al., 2011c; Ferreira et al., 2006). Since Faro Beach is the most urbanised and
146 exposed area of the Ria Formosa barrier island system, it is also the one with the higher potential risk
147 (Ferreira et al., 2016b).

148 Several management plans have been designed for Faro Beach (since the 1950's) but none of them
149 implemented to this day. The most recent and detailed management plan (Plano de Pormenor da
150 Praia de Faro) has as main goals to minimize the risk for people and goods, improve the use and the
151 habitability conditions at the area in harmony with the surrounding environment. For that, it proposes
152 to remove the occupation at risk and to maintain/improve the natural conditions of the ecosystem.
153 The proposed DRR measures, similar to the ones assessed/modelled here, include the partial removal
154 of houses at risk in combination with the nourishment of the beach and dune. The associated social
155 and economic implications of this plan have (so far) prevented its implementation.

156 **3. Emma storm**

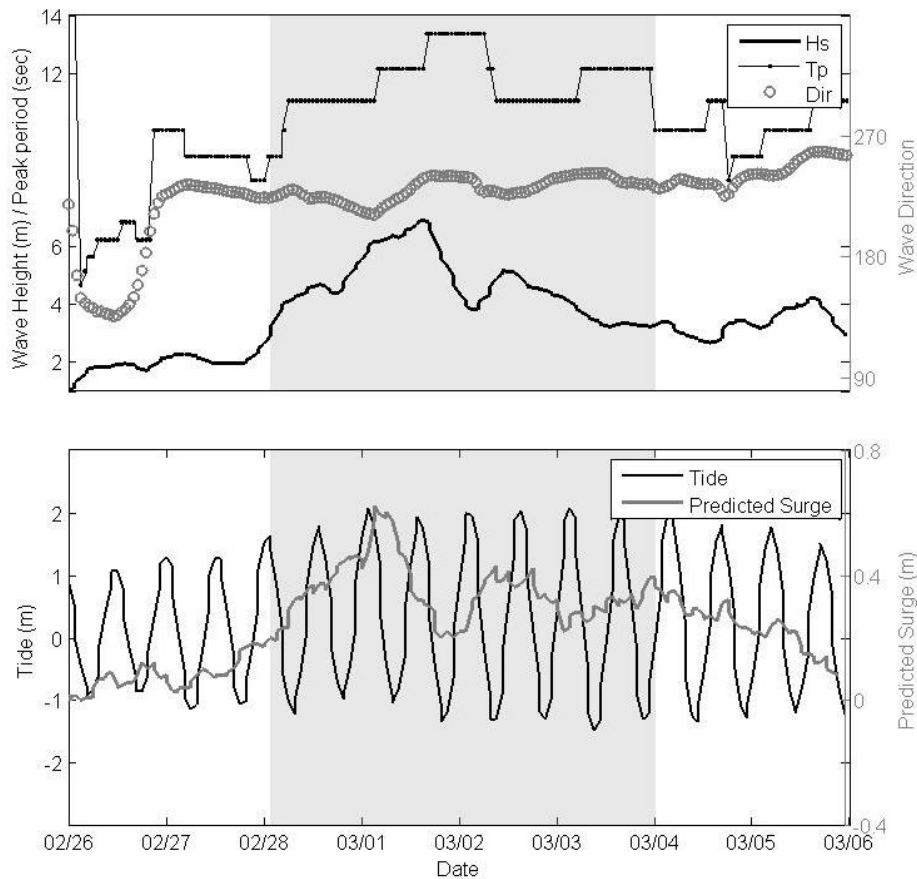
157 Emma storm (28 February to 3 March 2018) was formed SW of the Iberian Peninsula and had a track
158 (Figure 2) similar to some of the most energetic and devastating historical storms in the area (i.e. the
159 1941 windstorm and Xynthia in 2010; see Garnier et al. 2018). Hindcast data in the study area provided
160 by the Spanish Port Authority (Figure 3) show that close to Faro Beach the maximum Hs during the
161 storm was 6.9 m, with an associated peak period of 13.3 s. The wave direction during the storm varied

162 between 210° and 240° with an average direction of 230°. The maximum Hs corresponds to an
163 estimated return period of about 16 years (using the values expressed at Pires, 1998). Its coincident
164 occurrence with spring tides and the existence of a considerable storm surge (maximum values of
165 about 0.6 m at Huelva tide gauge), contributed to a total water level of about 2.1 m above mean sea
166 level, which corresponds to a water level return period on the order of 6-7 years, according to Carrasco
167 et al. (2012). Due to the interdependency of storm surge and Hs in the Gulf of Cadiz (Almeida et al.,
168 2012; Plomaritis et al., 2015), it can be assumed that the return period of the storm is mainly
169 controlled by the wave height. However, previous research has shown that the storm impact is highly
170 dependent on the timing of the storm in relation to the tidal stage (Plomaritis et al., 2018) and thus
171 the occurrence of high spring tides during the storm peak (Figure 3) may have contributed to the
172 enhancement of the storm effects.



173

174 Figure 2. Storm track of Emma storm (red) and of two of the most significant previous hazardous
 175 storms in the area (1941 storm in green and Xynthia storm in blue). Emma storm track was extracted
 176 from pressure maps collected from METEOGALICIA THREDDS server. Data are a combination of
 177 forecast predictions of 24 hours window.



178

179 Figure 3. Hindcast prediction of wave characteristics (significant wave height, peak period and wave
 180 direction) (top panel) and water level characteristics (tide and surge at Huelva, Spain) (bottom panel)
 181 for storm Emma. Shaded area presents the simulation period, similar to the one where $H_s > 3$ m (storm
 182 threshold).

183 The Emma storm had a strong erosive effect at Faro Beach and was also responsible for overwash at
 184 specific (and lowered) areas. While overwash was responsible for piling up water and sediment over
 185 roads, at car parks and house yards, the erosive character was responsible for the damage of walls
 186 and promenades, and threatened houses placed at the front line (Figure 4).

187



188



189

190 Figure 4. Examples of Emma storm effects at Faro Beach: seafront promenade and wall destroyed
191 behind the rip-rap seawall (upper images), overwashed roads and car parks with inland sediment
192 transport by wind and waves (lower images).

193 4. Methods

194 4.1. Beach surveying

195 Five beach profiles were surveyed at Faro Beach, during low tide, using a Real Time Kinematic Global
196 Navigation Satellite System, at 1 Hz, with a centimetre accuracy (equipment) and a decimetre
197 precision (associated to operator errors during survey), just before (26 Feb 2018) and at the end (02
198 Mar 2018) of the storm. The profiles location (named A to E, from West to East) is presented on Figure
199 1. The eroded volumes (in m^3/m) were computed by comparing the pre and post-storm profiles and
200 taking as lower limit 1 m MSL, since in some cases it was not possible to have data below this elevation
201 due to the prevailing tidal (and runup) conditions. On the 3 March 2018 a post-storm survey was
202 performed (by O. Ferreira) at the studied area to characterise the consequences of the storm, based

203 on visual observations and notes. The areas subject to overwash and associated damages were
204 recorded, as well as the position of the scarp/bluff line at the dune/berm and damages induced by
205 erosion. The position of the scarp/bluff line (or the most landward observed erosion when the scarp
206 was absent) was afterwards used to define the distance to houses and infrastructures in order to
207 determine if those assets were within the 'potential damage' and 'damage' conditions defined by the
208 approach (see details at the 'DSS and effectiveness assessment').

209 4.2. Modelling and BN approach

210 The hazard and impact estimations were undertaken with a combination of numerical simulations
211 using a multi-hazard morphodynamic model, XBeach (Roelvink et al., 2009) in surf beat mode, that
212 calculates the longwave runup, overwash and morphological changes (including erosion). XBeach is a
213 process based model with extensive application to storm conditions. Such model has been already
214 tested and validated for the study area (see Vousdoukas et al., 2012b) and further used within the
215 works of Poelhekke et al. (2016) and Plomaritis et al. (2018). However, the significant computational
216 cost of XBeach often limits its application into Early Warning Systems and Decision Support Systems
217 (DSS). An alternative methodology, which reduces computational costs on the operational window
218 allowing an immediate answer, is the use of a Bayesian Network approach (see Jäger et al., 2018 and
219 Poelhekke et al., 2016). This method uses a large number of pre-computed storm scenarios to train
220 the BN, providing a surrogate for the morphodynamic simulations in the DSS. A total of 232 different
221 storm conditions were then run and used to train the BN. These storms were selected to represent all
222 observed conditions and even expectable storms with higher return periods. A set of storms was
223 chosen for the interval between $3\text{ m} < H_s < 8.1\text{ m}$ (~50 year return period) with the selection limits for
224 all parameters (H_s , sea level including surge, and peak period) being available at Plomaritis et al. (2018;
225 Table 1). In order to introduce the effect of the nourishment (as a DRR measure), all storms needed
226 to be modeled again changing the beach morphology by including the nourishment. The data were
227 then used to build a DSS using the BN to surrogate the modelling. The BN can be accessed in order to
228 provide results for any incoming storm or to test the effectiveness of in place (or expected) DRR

229 measures. This approach was based on the source-pathway-receptor concept, with the addition of
230 consequences that were obtained from damage transfer functions. The DSS system used has been
231 already developed for Faro Beach and the procedure followed is further detailed in Poelhekke et al.
232 (2016) and Plomaritis et al. (2018). The boundary conditions of each storm (in this case average values
233 during the peak of the storm for wave height, peak period and water level) are represented in the BN
234 by separated nodes (variables) and each variable is divided in bins (e.g. wave heights and sea levels at
235 each 1 m intervals, peak periods at each 2 s intervals). The number of bins of each variable can vary
236 but the total range represents all possible boundary condition values. The ensemble of considered
237 bins (i.e. for each storm condition) are also referred (or can be considered) as 'states'.

238 Storm Emma impacts were computed in two ways:

- 239 a) by a baseline test ("Emma modelling") using as boundary conditions the wave and surge data
240 obtained from the hindcast model. The shaded area in Figure 1 represents the nearshore
241 XBeach model domain. For the model validation profiles A, B and C (within the XBeach model
242 domain) were used,
- 243 b) by applying the "Trained BN" introducing the peak storm average conditions (12 hours) as
244 input and directly obtaining the expected impacts from the BN solution for the most similar
245 range of conditions (set of bins or states) expressed by the BN.

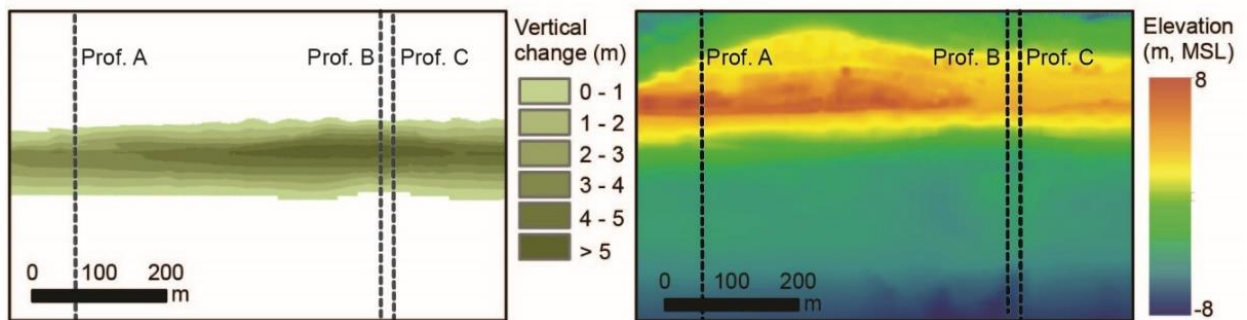
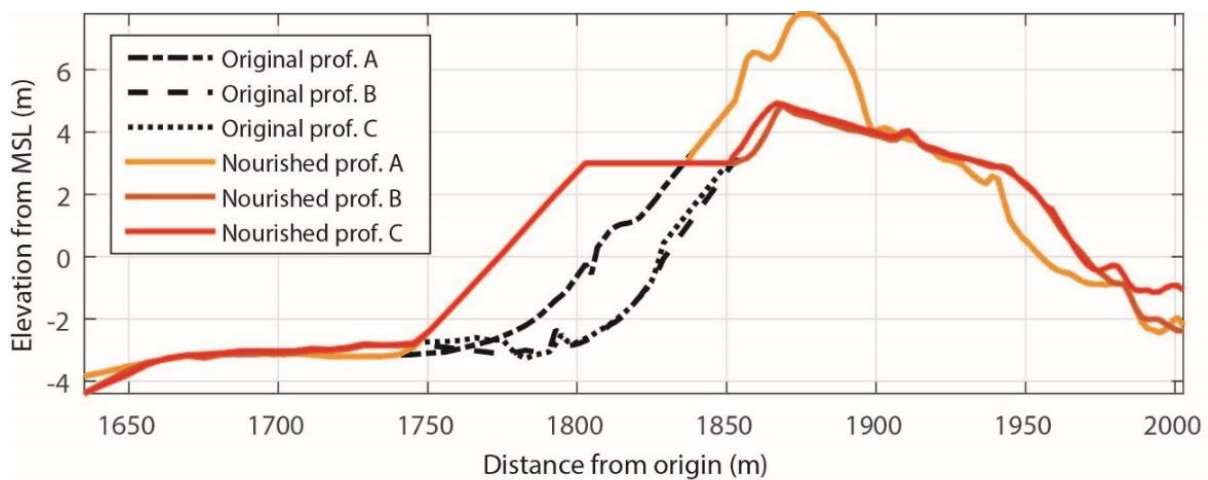
246 It must be stated that no rigid features have been implemented at the modelling. The permeable rip-
247 rap seawall that limits the upper beach at part of the study area (see Figure 4 upper images) was
248 incorporated by using an increased friction at the boundary between the beach and the dune/car
249 parking. The use of a hard layer at the model would completely avoid coastal retreat or damage behind
250 the rip-rap seawall, which would not fully represent the effect of this coastal protection at Praia de
251 Faro (see Figure 4, upper images).

252 4.3. DSS and effectiveness assessment

253 The DSS was applied in order to determine the potential consequences at Praia de Faro in terms of
254 expected damage to the considered receptors (i.e. houses and infrastructures) by overwash and
255 erosion, for a storm similar to Emma and four different scenarios:

- 256 A) Current situation (no DRR measure in place)
- 257 B) Beach nourishment including the construction of a circa 45 m wide berm (Figures 5 and 6)
- 258 C) Removal of the houses (Figure 6) placed at the ocean side of Faro Beach (between the main
259 road and the beach)
- 260 D) Beach nourishment (B) + House removal (C)

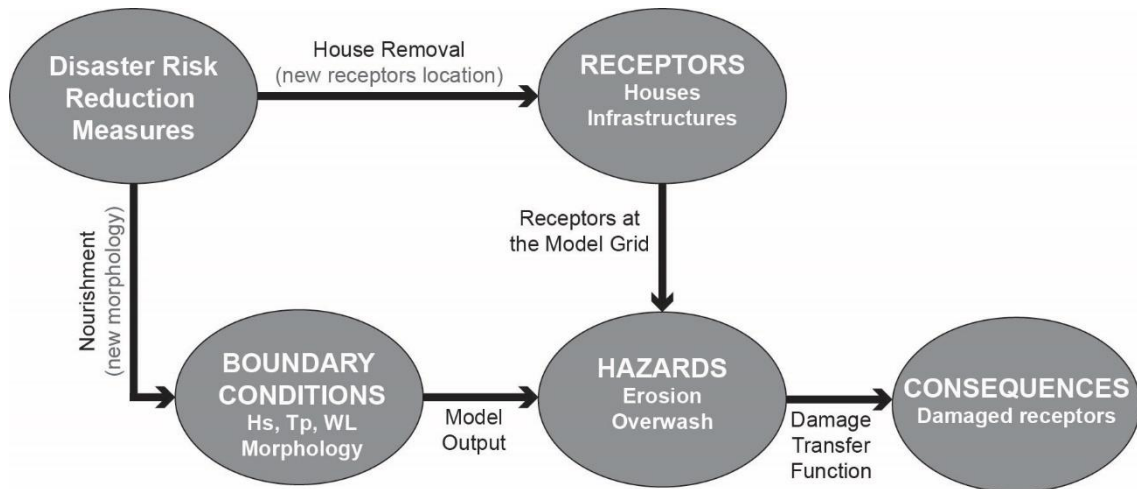
261 For the current approach, 'infrastructures' include the building environment (i.e. car parks, roads, and
262 promenades) except residential houses. The latter, together with bars, restaurants and hotels/hostels
263 were included into the broad classification of 'houses' (see Figure 1, lower panel).



264

265 Figure 5. (a) Original (black) and nourished (color) profiles along Faro Beach; (b) Vertical elevation
 266 differences between the replenished and the original beach topo-bathymetry for the model domain;
 267 (c) Original nearshore bathymetry of the model domain. Dashed lines shows the profile's location.

268



269

270 Figure 6. Design of the Decision Support System with the implementation of two Disaster Risk
 271 Reduction measures: Nourishment, changing the boundary conditions and the modelling outputs;
 272 House Removal, changing the receptors' location.

273 Overwash hazard was evaluated at the receptors (houses and infrastructures) using the maximum
 274 overwash discharge (Q) during the event. Specific overwash damage curves are not available for Faro
 275 Beach. Hence, a simple qualitative block damage curve was used with 2 threshold values to separate
 276 'safe', 'potential damage' and 'damage' to receptors. For discharges smaller than 1 m²/s the receptors
 277 are considered 'safe' while discharges equal or greater than 3 m²/s will cause 'damage'. For
 278 intermediate values, receptors were considered as 'potentially damaged' (see Plomaritis et al. 2018
 279 for details). Erosion hazard was evaluated for houses using the maximum erosion during an event at
 280 the house location and within two buffer zones surrounding them, one marked at 5 m radius and one
 281 at 10 m radius. The houses are considered to be 'damaged' when the vertical erosion is equal or
 282 exceeds 1.5 m at their location. The houses are considered to be 'safe' when the vertical erosion is
 283 less than 1.5 m at the 10 m buffer zone. For all other intermediate cases the houses are considered

284 'potentially damaged' (Plomaritis et al., 2018). For the case of erosion to infrastructures, a simpler
285 scheme was employed where only the erosion at the actual infrastructure location was considered.
286 For vertical erosion values equal or larger than 1.5 m an infrastructure is considered 'damaged', while
287 for smaller vertical erosion values the infrastructure is considered 'potentially damaged'. If no erosion
288 is observed the infrastructure is considered to be 'safe'.

289 The DRR effectiveness computation was performed by using an effectiveness index (*Ie*) for each DRR
290 intervention:

$$291 \quad Ie = 100 \% \times \frac{(\% \text{ damage current situation} - \% \text{ damaged with DRR})}{\% \text{ damage current situation}} \quad \text{Equation 1}$$

292 A zero (0%) value expresses that the DRR measure had no benefit when compared to the current
293 situation, while 100% indicates total risk prevention by the modeled DRR. Thus, the higher the value
294 of *Ie*, the higher the risk reduction capacity of the DRR measure, when compared to the initial
295 situation.

296 The *Ie* index was applied to scenarios B, C and D (against scenario A, current situation) by considering
297 'potential damage' and 'damage' infrastructures identified after modelling and BN use.

298 **5. Results**

299 **5.1. Emma storm impact and XBeach validation**

300 Emma storm produced the total removal of the beach berm and a maximum vertical erosion higher
301 than 2 m along the entire study area (Figure 7), exposing the rip-rap seawall and destroying some
302 existing infrastructures (e.g. seafront promenade, walls, stairs to access the beach). The volume
303 eroded from the upper part of the beach face (above 1 m MSL) is presented in Table 1. The measured
304 profiles seems to pivot around mean sea level or slightly above, and thus the measured values are
305 inferior to the total observed erosion of the upper beach profiles. It can be observed that along Faro
306 Beach the erosion volumes were similar, ranging from 51.6 m³/m to 60.3 m³/m, with an average value
307 of 56.3 m³/m. Differences on erosion values can be attributed to the initial profiles variability, namely

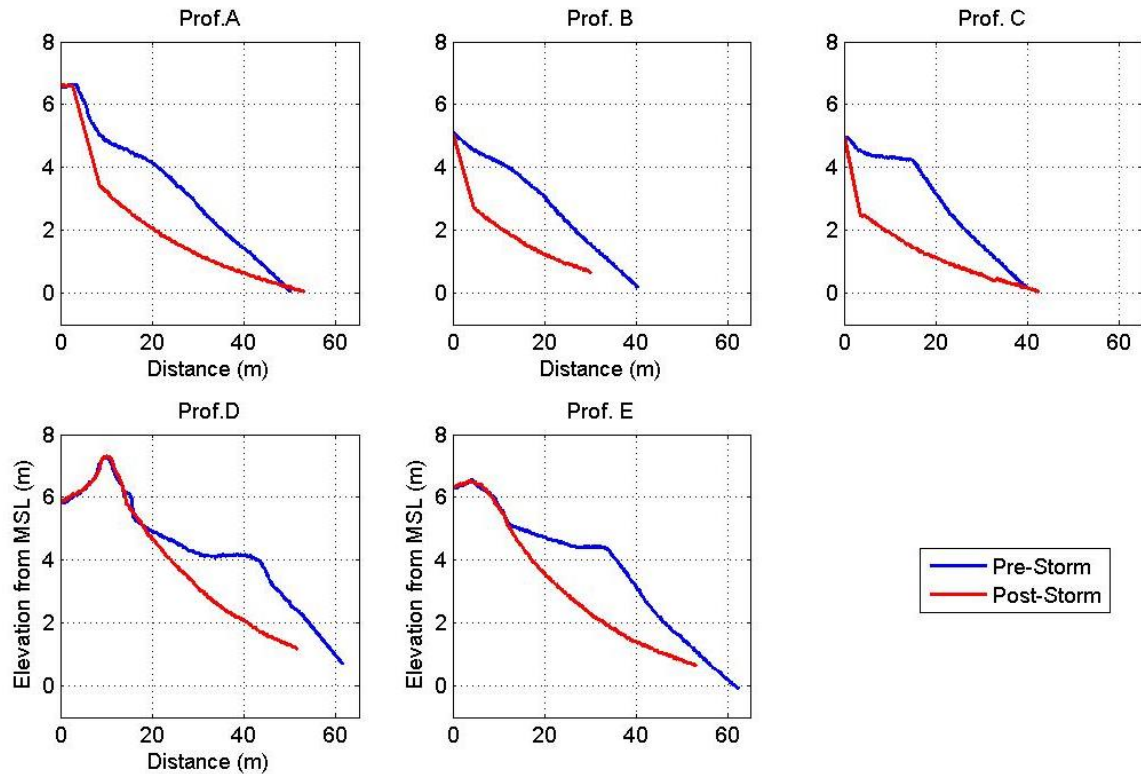
308 the presence of beach cusps. Some profiles (e.g. C and D) are also backed by a rip-rap seawall and a
309 hard surface (car parks), which may also affect their response to a storm.

310 Table 1. Sediment volume (m³/m) eroded from the upper beach (above 1 m MSL) during Emma storm.

	Profile A	Profile B	Profile C	Profile D	Profile E
Eroded volume	60.3	51.6	58.7	52.7	58.1

311

312 Overwash has been observed along the study area, mainly at car parks and at some other locations to
313 the eastern limit of the studied area. The higher dunes at the west prevented overwash. Apart from
314 bringing a large amount of sediment to the road and house yards, overwash also caused minor
315 damages to a hotel, restaurants and private houses, despite the fact that several of them have been
316 beforehand protected with sand bags.

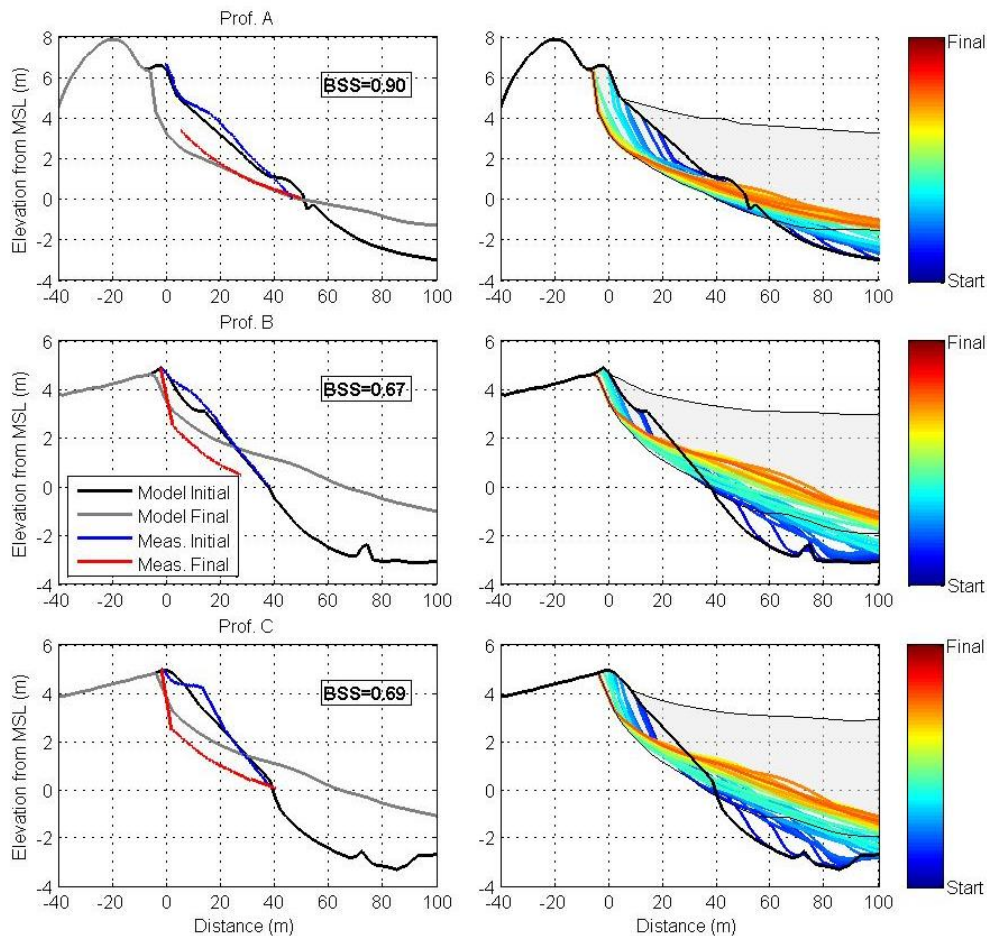


317

318 Figure 7. Measured pre- and post-storm profiles along Praia de Faro for the storm Emma. Profile
 319 locations are given in Figure1.

320 Using the XBeach modelling results and the measured data (post-storm profiles A to C), a validation
 321 of the XBeach model was undertaken (Figure 8). The Brier skill scores (BSS) obtained were between
 322 0.67 and 0.9, which are considered Excellent for morphodynamic modeling simulations (Sutherland et
 323 al., 2004), reflecting a good ability of the model to simulate the morphological response. Similar to the
 324 measured profiles, the model results presented alongshore quasi-uniform erosion over the study area,
 325 which agree with visual observations during the post-storm survey. Close to the dune crest the vertical
 326 erosion values are close to 1.5 m with an absolute maximum of about 2.5 m at profile A. The model
 327 outputs show significant erosion of the dune (or the highest elevation; e.g. car parks or seafront
 328 promenade) along the central and western parts. These results were also confirmed during the post-
 329 storm visual survey.

330 For the given conditions, and for both the baseline and the Trained BN, the DSS estimated limited
331 damages by erosion to the houses (5%-3%; Table 2) and infrastructures (6%; Table 3) located at the
332 ocean western area of Faro Beach. Most of the houses and infrastructures are considered safe (64%-
333 73% and 81%-94%, Tables 2 and 3). The remaining houses and infrastructures are classified as
334 potentially damaged and those correspond to the occupation located at the first line of the beach
335 front. The classification as potentially damaged house is not an indicator of actual damage but of the
336 existence of strong vertical erosion at a horizontal distance near the houses (< 10 m). Due to the
337 damage transfer function applied to the infrastructure erosion (no buffer zones) and the scarp like
338 final profiles predicted by the model, no potentially damaged infrastructures were estimated. All the
339 damaged infrastructures are located in the car parking zone. During the post-storm field survey, it was
340 observed that no houses have been destroyed but several (27 houses and bars) have been identified
341 within the potentially damaged condition (nearby strong vertical erosion), representing 16% of the
342 total houses under the modelling domain. The inexistence of damaged houses and the reduced
343 number of potentially damaged houses (when compared to the modelling and BN predictions) was
344 most probably due to the protective action of the rip-rap seawall placed under the dune crest in front
345 of the more severely affected area, which reduced shoreline retreat and avoided house destruction.
346 That rip-rap seawall was only partially considered within the modelling through the use of an increased
347 friction at its position, allowing wave impact to occur behind the structure, but probably not fully
348 representing its protective action.



349

350 Figure 8. XBeach model validation (left panels) for profiles A to C. Profile evolution during the storm
 351 (right panels) for the same profiles. Shaded areas on the right panels represent the water envelope.

352 Regarding infrastructures, 3% of the total longshore model domain presented infrastructure damages,
 353 namely stairs and promenades (see Figure 4), while about 11% could be considered potentially
 354 damaged (vertical erosion at the infrastructure but without collapse). These values are in good
 355 agreement with the ones expressed by the modelling and trained BN (Table 3). The protective effect
 356 of the rip-rap seawall did not completely avoid infrastructure destruction since it is a permeable
 357 seawall and most of these structures were placed in front (seaward), above or immediately behind
 358 the rip-rap seawall and thus have been directly affected by the storm.

359 It is visible in Figure 8 (Profiles B and C) that limited overwash occurred at some locations, since the
 360 maximum water level exceeded the maximum profile elevation. The model predicts overwash at the
 361 central and eastern parts of the study area, which was confirmed at the post-storm field survey (see

362 Figure 4). Along the car parking area, the predicted mean overwash water flux was 0.22 m²/s with
 363 maximum values of 0.7 m²/s at the western edge of the car park. For overwash, the BN/Model
 364 estimated damages on 0% of the houses, 98%-99% of safe houses and 1%-2% (Table 4) of potentially
 365 damaged houses (overwash velocities between 1-3 m/s), while for infrastructures only the BN predicts
 366 damages or potential damages and for only 4% of the area. The field survey allowed the identification
 367 of minor damages that could be partially attributed to overwash (e.g. scour of the pavement
 368 surrounding the lamppost at the central image of Figure 4). Nevertheless, several infrastructures and
 369 houses (hotels and restaurants mainly) were directly overwashed (see Figure 4 for examples),
 370 suggesting a slight underestimation of the overwash.

371 Table 2. Synthesis of Safe (S), Potentially Damaged (DP) and Damaged (D) houses for Faro Beach,
 372 according to DSS, for erosion hazard, predicted by the trained BN and by the Emma storm modeling,
 373 for the 4 tested scenarios (A – current situation; B - beach nourishment; C – house removal; D = B +
 374 C).

DRR scenarios	A			B			C			D		
	S	PD	D	S	PD	D	S	PD	D	S	PD	D
Trained BN	64	31	5	100	0	0	89	11	0	100	0	0
Emma Modelling	73	24	3	97	3	0	91	9	0	100	0	0

375

376 Table 3. Synthesis of Safe (S), Potentially Damaged (DP) and Damaged (D) infrastructures for Faro
 377 Beach, according to DSS, for erosion hazard, predicted by the trained BN and by the Emma storm
 378 modeling, for the 4 tested scenarios (A – current situation; B - beach nourishment; C – infrastructure
 379 removal; D = B + C).

DRR scenarios	A			B			C			D		
	S	PD	D	S	PD	D	S	PD	D	S	PD	D
Trained BN	81	13	6	97	3	0	94	6	0	99	1	0

Emma Modelling	94	0	6	100	0	0	100	0	0	100	0	0
-------------------	----	---	---	-----	---	---	-----	---	---	-----	---	---

380

381 Table 4. Synthesis of Safe (S), Potentially Damaged (DP) and Damaged (D) houses for Faro Beach,
 382 according to DSS, for overwash hazard, predicted by the trained BN and by the Emma storm modeling,
 383 for the 4 tested scenarios (A – current situation; B - beach nourishment; C – house removal; D = B +
 384 C).

DRR scenarios	A			B			C			D		
	S	PD	D	S	PD	D	S	PD	D	S	PD	D
Trained BN	98	2	0	100	0	0	100	0	0	100	0	0
Emma Modelling	99	1	0	100	0	0	100	0	0	100	0	0

385

386 Table 5. Synthesis of Safe (S), Potentially Damaged (DP) and Damaged (D) infrastructures for Faro
 387 Beach, according to DSS, for overwash hazard, predicted by the trained BN and by the Emma storm
 388 modeling, for the 4 tested scenarios (A – current situation; B - beach nourishment; C – house removal;
 389 D = B + C).

DRR scenarios	A			B			C			D		
	S	PD	D	S	PD	D	S	PD	D	S	PD	D
Trained BN	96	4	4	100	0	0	100	0	0	100	0	0
Emma Modelling	100	0	0	100	0	0	100	0	0	100	0	0

390

391 5.2. DRR measures effectiveness

392 The most effective DRR measure regarding erosion promoted by Emma storm is the one that considers
 393 both nourishment and house removal, with effectiveness values on the protection of
 394 houses/infrastructures always near 100% (Table 6). The less effective DRR measure is the partial house
 395 removal alone that, according to the used prediction model, is still effective for 54% to 100% of the

396 cases (Table 6). The beach nourishment alone presents high values of effectiveness (77% to 100%,
 397 Table 6 and Figure 9), regarding the minimization of damages (or potential damages) caused by
 398 erosion.

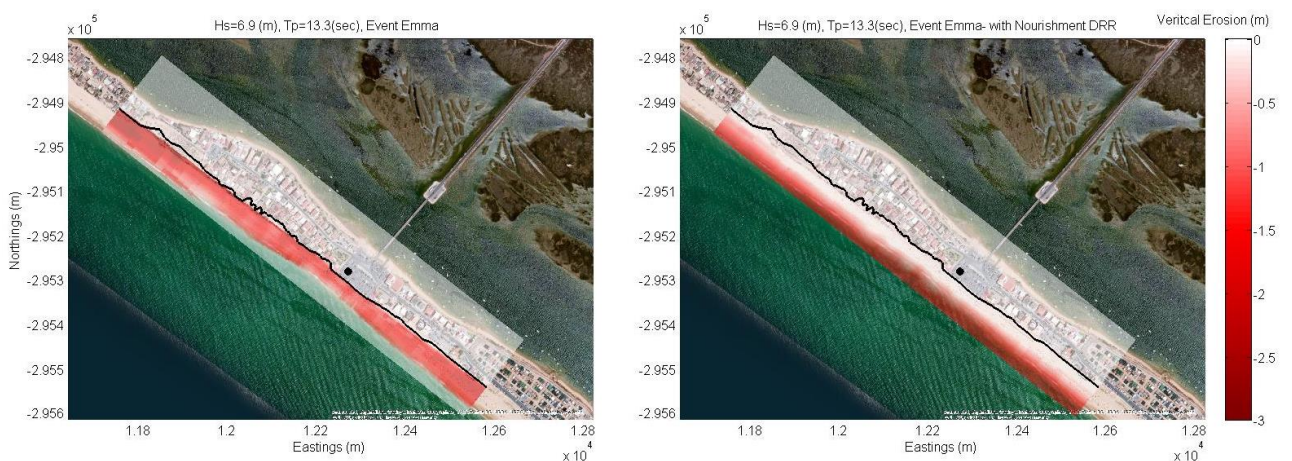
399 Regarding the damages (or potential damages) associated with the overwash all DRR are 100%
 400 effective, for all considered scenarios. The baseline test and the trained BN presented similar
 401 effectiveness results. The observed differences are mainly related to the consequences predicted for
 402 the current situation (scenario A).

403 Table 6. Effectiveness regarding erosion (*I_e* in %), predicted by the trained BN and by the Emma storm
 404 modeling for the tested DRR measures (B - beach nourishment; C – house removal; D = B + C).

405 Potentially Damaged (PD) and Damaged (D) houses/infrastructures for Faro Beach.

DRR scenarios	B		C		D	
	PD	D	PD	D	PD	D
Trained BN	100/76.9	100/100	64.5/53.6	100/100	100/83.3	100/100
Emma Modelling	87.5/100	100/100	62.5/100	100/100	100/100	100/100

406



407

408 Figure 9. Example of output from the Emma modelling for vertical erosion under current
 409 morphological conditions (left image) and after beach nourishment (right image). The black line

410 represents the limit between the human occupation and the beach/dune. Red values landward or
411 near that line (< 10 m) represent damage or potential damage to houses/infrastructures.

412 **6. Discussion**

413 Governments and managers are increasingly interested in identifying where DRR measures can be
414 effectively used. There is, however, very little consensus as to what constitutes effective and adequate
415 adaptation (e.g. for climate change) and how to measure it (Craft and Fisher, 2016). As for adaptation,
416 the same occurs on the evaluation of risks and associated reduction measures, including legislation
417 (see Drejza et al. 2011). It is therefore challenging to assess the effectiveness of DRR measures, which
418 can be done in several different ways. Those range from the simple use of emails or interviews to ask
419 the population about the effectiveness of coastal erosion management (e.g. Luo et al., 2015) to the
420 quantification of the protection induced by a specific risk reduction measure (e.g. wave energy
421 dissipation by coral reefs; Ferrario et al., 2014). Craft and Fisher (2016) stated that one metric currently
422 used to assess effectiveness is the measurement of vulnerability and resilience. In this work we used
423 a similar concept and determined the effectiveness of DRR measures against overwash and storm
424 induced erosion by computing an effectiveness index directly related to the risk reduction provided
425 by each measure. This index (and overall methodology) can be applied beforehand allowing coastal
426 managers to test the DRR measures and to have an informed decision towards the implementation of
427 the most effective management approach.

428 **6.1. Modelling validation and errors**

429 The modelling validation proved that the obtained results with XBeach are reliable for Faro Beach and
430 Emma storm (see Figure 8). Predicted erosion and overwash by Emma modelling and trained BN, as
431 well as the estimated damage (or potential damage) of houses and infrastructure (Tables 2 to 5,
432 scenario A), are generically in agreement with field observations. A relatively small part of the
433 houses/infrastructures were effectively damaged, mostly by erosion, as modelled. The predicted
434 potential damage (mainly by erosion) of 24-31% of the houses and 13% of the infrastructures was also

435 observed since part of the houses (16%) and infrastructures (11%) placed at the first occupation row
436 (over the dune) was considered within the potentially damaged boundaries, during the post-storm
437 survey. The validation performed immediately after the storm allowed to verify that the model
438 predictions (percentages) and observation for damage or potentially damaged houses/infrastructures
439 differed mostly in less than 10%, reaching a maximum of 15% (at the potentially damaged houses).
440 This can be regarded as an overall measure of the model uncertainty and several factors might
441 contribute to it. One such factor is that the BN, and consequently the DSS, always starts from the same
442 initial bathymetry/topography or from a limited selection of initial bathymetries, and thus differences
443 between the measured and the initial model profiles can exist. This is a limitation (from an
444 assumption) of the current methodology that can be solved in the future by integrating different topo-
445 bathymetric conditions at the modelling. It can be seen in Figure 8 that differences between initial
446 modelled and measured profiles are relatively small and mainly due to alongshore cusps that can be
447 frequently observed in the area. In the present case, volume differences between the initial profiles
448 varied between 8 and 16 m³/m, which represents a change of 14-28% of the average eroded volume,
449 and thus that can be assumed as the average error associated to the variability between measured
450 and modelled initial profiles. A potential improvement of the method will be to consider different
451 possible initial morphologies and analyse the potential storm consequences under a range of
452 morphologies.

453 Differences between the final model and the measured profiles could also be due to the presence of
454 a protection work (permeable rip-rap seawall) that is present in the area but has been just partially
455 introduced in the model. Profiles B and C are backed by the car parking area of Praia de Faro and by
456 the seafront promenade, which are protected by large boulders (rip-rap seawall) buried in the sand.
457 During the present event a large portion of the seafront promenade was undermined and destroyed
458 by the storm (see Figure 4), however, this behaviour is not fully captured by the post-storm profiles
459 (due to difficulties on surveying over the boulders). Similarly, part of the eroded area in Profile A
460 presents contrasting geotechnical properties relatively to a dune as it is composed by a more

461 compacted sediment layer with a large content of clays. That may explain the greater dune retreat
462 simulated by the model compared to the observations. In addition, the boulders and resistant soils
463 increased the wave reflection, which can in turn increase the offshore transport of sand and further
464 lower the beach profiles. This might be responsible for the higher expressed vertical erosion at the
465 measured profiles when compared to the modelled ones.

466 The slight underestimation of the overwash (when qualitatively compared to the observed overwash
467 and consequences) can result from the non-inclusion of short wave induced overwash (only infragravity
468 wave overwash is predicted by the model) and also because the resolution of the surge model may
469 not be enough to fully capture the surge magnitude and, consequently, the total water level. The
470 absence of a local tidal gauge does not permit a more thorough validation of the model.

471 Finally, a source of inaccuracy on the model prediction is the wave and surge prediction models
472 resolution. The overall final result from the morphodynamic model highly depends on the input values
473 (from the predictions) and thus improved (and validated) regional wave and surge models are highly
474 important for the achievement of good and representative results. A validated model train that would
475 better downscale the regional prediction could result in an even more accurate representation of the
476 storm consequences. Nevertheless, as already stated, the observed uncertainty of expected damages
477 was relatively small, with differences between modelled and field observations being always below
478 15% of the total maximum potential damage and in most cases between 5 and 10%, which can be
479 considered a good performance of the model for such a high energy event as the Emma storm.

480 6.2. DRR effectiveness

481 The modelling results can be used to further train the BN and to improve the results of the DSS.
482 However, since the BN is a surrogate of the modelling and uses bins that represent similar storm
483 conditions and morphologies, a storm at the BN is not represented by its exact values and respective
484 modelling but by the overall modelled erosive conditions (and impacts) associated to the bins (e.g. H_s ,
485 T_p , sea level) within which that storm fits (Jäger et al., 2018; Poelhekke et al., 2016). Thus, damage

486 and potentially damage values for overwash and erosion must be seen as representative values for
487 storms with similar characteristics and will incorporate a certain level of variance. However, given the
488 fact that the storm characteristics are probably a result of an operational forecast model with
489 associated prediction errors, the BN approach in a DSS provides a more robust prediction since it
490 informs about the intensity of the hazards and associated damages based on a number of similar
491 storms. Similarly, the effectiveness of the DRRs is calculated based on the same principles.

492 All modelled DRR have a total effectiveness (100%; Tables 4 and 5) in reducing overwash impacts since
493 the level of modelled (and field observed) overwash was not extreme at this storm. The most effective
494 DRR measure to reduce the damages associated to erosion is the combination of nourishment and
495 house removal, followed by the nourishment alone (Table 6). For this storm (circa 16 year return
496 period) these two measures have almost the same effectiveness level. This is however probably not
497 valid for storms with higher return period where the nourished berm can be fully eroded.

498 The trained BN predicts always more damages than the single Emma storm modelling, however both
499 tests provide similar tendencies with increased erosion hazards and consequences in comparison to
500 overwash. This results from the inclusion of several tested storms under the generic conditions that
501 represent the Emma storm within the BN. This makes it a stricter tool for calculating potential
502 damages and effectiveness of DRR measures. The BN outcome has, however, some level of
503 uncertainty since each storm is then represented by a set of bins (or stages) with some variability. For
504 instance, at the used BN (see Plomaritis et al., 2018) the wave height bins have intervals of 1 m, with
505 the Emma storm being represented by wave heights ranging from 6 m to 7 m. That can be minimised
506 by increasing the training of the BN for each state or by detailing the discretization intervals (e.g. each
507 half meter), which (for both cases) requires a higher number of modelling simulations.

508 The obtained DRR effectiveness for the nourishment (and nourishment + house removal) considers
509 that the beach morphology is always equal to the one immediately after the nourishment
510 intervention, representing a maximum protective effect. This effect diminishes with time since there

511 will be sand removal by longshore transport on an average of about 100,000 m³/year (Santos et al.,
512 2017). Thus, the presented DRR effectiveness assessment considers that the nourishment is
513 maintained over time. It would be also possible (not presented at this work) to estimate the beach
514 nourishment reduction with time and to simulate the decrease in effectiveness in order to provide the
515 coastal manager with a clear indication of when a new intervention should be performed.

516 Regarding partial house removal, the DRR effectiveness assessment considers that there is no dune
517 recovery with time (natural or human incremented). Thus, although probably correct for the moment
518 immediately after the DRR intervention, the effectiveness of the measure will probably increase as
519 dunes naturally grow with time. Natural dune recovery after house removal has been observed at the
520 area (after interventions in 1987 and 2015) and it is expected to occur if this measure is further
521 implemented.

522 6.3. The DSS in coastal management

523 The results expressed along this work prove that it is possible to determine and compare the
524 effectiveness of different coastal management actions regarding their potential to minimise coastal
525 risks. The tested management actions are not restricted to the reduction of the hazard by minimising
526 the impact of the storms at the pathway (e.g. beach and dune nourishment) but also include the
527 reduction of risk by changing the receptors (e.g. new land use or improved management), allowing
528 the test of multi-disciplinary approaches. That can be done ex-ante, for specific storms (as here
529 represented) or for a large set of pre-defined conditions. The complex and time-expensive modelling
530 can be integrated into a BN that can be retaken, when needed, to reassess the effectiveness of a new
531 defined condition. This decision support system can be adapted to any sandy coastal area and
532 afterwards implemented. It can also be used for a vast set of potential measures, including the ones
533 here tested (house removal and beach nourishment) but also dune recovery, detached breakwaters,
534 placement of submerged bars, etc. By using the here proposed effectiveness method and index, the
535 managers can have a clear idea of the effects of each measure beforehand and evaluate the cost-

536 benefit. Thus, they have the possibility of taking an informed option towards the improvement of
537 coastal management actions at their region. It will allow to reduce budgets and optimise costs, since
538 an approach of trial and error can be made a priori, avoiding (or minimizing) the costs of
539 implementation of a given measure. For instance, several nourishment designs can be tested in order
540 to define the one that minimizes the risk to a desired level (using the effectiveness index) at a lower
541 cost. It also allows, on natural systems, to better define set-back lines for storm effects associated to
542 a pre-established return period.

543 A full cost-benefit analysis of coastal management alternatives is desirable and could be performed
544 jointly with the proposed approach. By including such analysis, it is possible to simulate the benefits
545 for the economy of a coastal area and, as well, the benefits for the ecosystem services provided by
546 the coastal zone, thus contributing to a better assessment of the impact of the management actions.

547 **7. Conclusions**

548 This work proposes the use of a validated numerical model or of a surrogate trained Bayesian network
549 to determine the potential impacts of storms at coastal areas, with and without disaster risk reduction
550 measures, and to further evaluate the success of such measures. It also presents a new effectiveness
551 index to evaluate, in a simple and comparative way, the effect of the measures. The model, the
552 Bayesian network and the effectiveness index were tested at Faro Beach, for Emma storm, a 16 year
553 return period storm that caused infrastructure damage and threatened the occupation (houses, bars
554 and hotels) mostly due to erosion but also (to a minor extent) by overwash. The results proved that
555 the use of beach nourishment (environmental based solution) alone or jointly with partial house
556 removal (societal based solution) would reduce the impacts of the tested storm to a residual level.
557 This approach represents, to our knowledge, the first attempt to demonstrate the effectiveness of a
558 coastal DSS against a specific and well-documented high-energy storm. The methodology is given as
559 example for further application in the future at global level, in order to better identify and test coastal
560 management measures that are effective in reducing risk to coastal populations. As demonstrated,

561 the methodology includes physical drivers (waves, sea level) and human occupation and allows testing
562 both environmental and societal based coastal management actions, jointly or separately. Such
563 approach will also help to optimise resources, which is in turn a factor of paramount relevance taking
564 into consideration the potential increase of coastal risks due to climate change (i.e. sea level rise and
565 increased frequency of extreme sea levels) and the increment of human occupation at coastal areas.

566 **Acknowledgements**

567 The authors would like to acknowledge Luisa Bon de Sousa and Margarida Ramires for the data
568 obtained at the fieldwork surveys. Susana Costas was funded through the “FCT Investigator” program
569 (ref. IF/01047/2014). This work was supported by the European Community's 7th Framework
570 Programme through the grant to RISC-KIT (“Resilience increasing Strategies for Coasts - Toolkit”),
571 contract no. 603458; projects EVREST (PTDC/MAR-EST/1031/2014) and EW-COAST (ALG-LISBOA-01-
572 145-FEDER-028657); and the Portuguese Science Foundation (FCT) through the grant
573 UID/MAR/00350/2013 attributed to CIMA of the University of Algarve.

574 **References**

- 575 Almeida L.P., Ferreira Ó., Pacheco A., 2011a. Thresholds for morphological changes on an exposed
576 sandy beach as a function of wave height. *Earth Surface Processes and Landforms*. 36, 523-
577 532.
- 578 Almeida L.P., Ferreira O., Voudoukas M.I., Dodet G., 2011b. Historical variation and trends in
579 storminess along the Portuguese South Coast. *Nat. Hazards Earth Syst. Sci.* 11, 2407-2417.
- 580 Almeida L.P., Ferreira Ó., Taborda R., 2011c. Geoprocessing tool to model beach erosion due to
581 storms: application to Faro beach (Portugal). *Proceedings of the 11th International Coastal*
582 *Symposium*. SI 64. *Journal of Coastal Research*, Szczecin, Poland, pp. 1830-1834.
- 583 Almeida L.P., Voudoukas M.V., Ferreira Ó., Rodrigues B.A., Matias A., 2012. Thresholds for storm
584 impacts on an exposed sandy coastal area in southern Portugal. *Geomorphology*. 143–144, 3-
585 12.

586 Aretano R., Parlagreco L., Semeraro T., Zurlini G., Petrosillo I., 2017. Coastal dynamics vs beach users
587 attitudes and perceptions to enhance environmental conservation and management
588 effectiveness. *Marine Pollution Bulletin*. 123, 142-155.

589 Barquet K., Dickin S.K., Meijer J.J., Dastgheib A., 2018. Testing RISC-KIT's integrated approach for
590 assessing Disaster Risk Reduction measures on the coast of Kristianstad, Sweden. *Coastal*
591 *Engineering*. 134, 203-211.

592 Bertin X., Bruneau N., Breilh J.-F., Fortunato A.B., Karpytchev M., 2012. Importance of wave age and
593 resonance in storm surges: The case Xynthia, Bay of Biscay. *Ocean Modelling*. 42, 16-30.

594 Bennington B., Farmer E.C., 2015. In: Bret Bennington, J., Christa Farmer, E. (Eds.), *Learning From the*
595 *Impacts of Superstorm Sandy*. Academic Press. Elsevier, pp. 123.

596 Bolle A., das Neves L., Smets S., Mollaert J., Buitrago S., 2018. An impact-oriented Early Warning and
597 Bayesian-based Decision Support System for flood risks in Zeebrugge harbour. *Coastal*
598 *Engineering*. 134, 191-202.

599 Brown J.M., Phelps J.J.C., Barkwith A., Hurst M.D., Ellis M.A., Plater A.J., 2016. The effectiveness of
600 beach mega-nourishment, assessed over three management epochs. *Journal of*
601 *Environmental Management*. 184, 400-408.

602 Burcharth H.F., Lykke Andersen T., Lara J.L., 2014. Upgrade of coastal defence structures against
603 increased loadings caused by climate change: A first methodological approach. *Coastal*
604 *Engineering*. 87, 112-121.

605 Carrasco A.R., Ferreira Ó., Matias A., Freire P., 2012. Flood hazard assessment and management of
606 fetch-limited coastal environments. *Ocean & Coastal Management*. 65, 15-25.

607 Ciavola P., Ferreira O., Haerens P., Van Koningsveld M., Armaroli C., Lequeux Q., 2011a. Storm impacts
608 along European coastlines. Part 1: The joint effort of the MICORE and ConHaz Projects.
609 *Environmental Science & Policy*. 14, 912-923.

610 Ciavola P., Ferreira O., Haerens P., Van Koningsveld M., Armaroli C., 2011b. Storm impacts along
611 European coastlines. Part 2: lessons learned from the MICORE project. *Environmental Science*
612 & Policy. 14, 924-933.

613 Clay P.M., Colburn L.L., Seara T., 2016. Social bonds and recovery: an analysis of Hurricane Sandy in
614 the first year after landfall. *Marine Policy*. 74, 334–340.

615 Costa M., Silva R., Vitorino J., 2001. Contribuição para o estudo do clima de agitação marítima na costa
616 Portuguesa. II Jornadas Portuguesas de Engenharia Costeira e Portuária, Sines, Portugal

617 Craft B., Fisher S., 2016. Measuring effective and adequate adaptation. London: International Institute
618 for Environment and Development.

619 Drejza S., Bernatchez P., Dugas C., 2011. Effectiveness of land management measures to reduce
620 coastal georisks, eastern Québec, Canada. *Ocean & Coastal Management*. 54, 290-301.

621 Ferrario F., Beck M.W., Storlazzi C.D., Micheli F., Shepard C.C., Airolidi L., 2014. The effectiveness of
622 coral reefs for coastal hazard risk reduction and adaptation. *Nature Communications*. 5, 3794.

623 Ferreira Ó., Garcia T., Matias A., Taborda R., Dias J.A., 2006. An integrated method for the
624 determination of set-back lines for coastal erosion hazards on sandy shores. *Continental Shelf*
625 *Research*. 26, 1030-1044.

626 Ferreira Ó., Matias A., Pacheco A., 2016a. The East Coast of Algarve: a Barrier Island Dominated Coast.
627 *Thalassas*. 32, 75-85.

628 Ferreira O., Viavattene C., Jiménez J., Bole A., Plomaitis T., Costas S., et al., 2016b. CRAF phase 1, a
629 framework to identify coastal hotspots to storm impacts. FLOODrisk 2016 - 3rd European
630 Conference on Flood Risk Management. 7. E3S Web Conf., Lyon, France, pp. 1-9.

631 Ferreira O., Viavattene C., Jiménez J.A., Bolle A., das Neves L., Plomaritis T.A., et al., 2018. Storm-
632 induced risk assessment: Evaluation of two tools at the regional and hotspot scale. *Coastal*
633 *Engineering*. 134, 241-253.

634 Garnier E., Ciavola P., Spencer T., Ferreira O., Armaroli C., McIvor A., 2018. Historical analysis of storm
635 events: Case studies in France, England, Portugal and Italy. *Coastal Engineering*. 134, 10-23.

636 Huguet J.-R., Bertin X., Arnaud G., 2018. Managed realignment to mitigate storm-induced flooding: A
637 case study in La Faute-sur-mer, France. *Coastal Engineering*. 134, 168-176.

638 Jäger W.S., Christie E.K., Hanea A.M., den Heijer C., Spencer T., 2018. A Bayesian network approach
639 for coastal risk analysis and decision making. *Coastal Engineering*. 134, 48-61.

640 Kantha L., 2013. Classification of hurricanes: lessons from Katrina, Ike, Irene, Isaac and Sandy. *Ocean*
641 *Engineering*. 70, 124–128.

642 Kombiadou K., Matias A., Carrasco R., Ferreira Ó., Costas S., Vieira G., 2018. Towards Assessing the
643 Resilience of Complex Coastal Systems: Examples from Ria Formosa (South Portugal). In: Shim
644 J-S, Chun I, Lim HS, editors. *International Coastal Symposium (ICS) 2018*. 85. *Journal of Coastal*
645 *Research*, Busan, Republic of Korea, pp. 646-650.

646 Link L.E., 2010. The anatomy of a disaster, an overview of Hurricane Katrina and New Orleans. *Ocean*
647 *Engineering*. 37, 4–12.

648 López-Rodríguez F., Rosado D., 2017. Management effectiveness evaluation in protected areas of
649 southern Ecuador. *Journal of Environmental Management*. 190, 45-52.

650 Luo S., Cai F., Liu H., Lei G., Qi H., Su X., 2015. Adaptive measures adopted for risk reduction of coastal
651 erosion in the People's Republic of China. *Ocean & Coastal Management*. 103, 134-145.

652 Masselink G., Castelle B., Scott T., Dodet G., Suarez S., Jackson D., et al., 2016. Extreme wave activity
653 during 2013/2014 winter and morphological impacts along the Atlantic coast of Europe.
654 *Geophysical Research Letters*. 43, 2135-2143.

655 Neal W.J., Pilkey O.H., Cooper J.A.G., Longo N.J., 2018. Why coastal regulations fail. *Ocean & Coastal*
656 *Management*. 156, 21-34.

657 Oliveira T.C.A., Neves M.G., Fidalgo R., Esteves R., 2018. Variability of wave parameters and Hmax/Hs
658 relationship under storm conditions offshore the Portuguese continental coast. *Ocean*
659 *Engineering*. 153, 10-22.

660 Perini L., Calabrese L., Lorito S., Luciani P., 2015. Coastal flood risk in Emilia-Romagna (Italy): the sea
661 storm of February 2015. In: Coastal and Maritime Mediterranean Conference, Edition 3, pp.
662 225–230.

663 Pires H.O., 1998. Project INDIA. Preliminary report on wave climate at Faro. Instituto de Meteorologia,
664 IST, Lisboa, Portugal.

665 Plomaritis T.A., Benavente J., Laiz I., Del Río L., 2015. Variability in storm climate along the Gulf of
666 Cadiz: the role of large scale atmospheric forcing and implications to coastal hazards. *Climate*
667 *Dynamics*. 45, 2499-2514.

668 Plomaritis T.A., Costas S., Ferreira Ó., 2018. Use of a Bayesian Network for coastal hazards, impact and
669 disaster risk reduction assessment at a coastal barrier (Ria Formosa, Portugal). *Coastal*
670 *Engineering*. 134, 134-147.

671 Poelhekke L., Jäger W.S., van Dongeren A., Plomaritis T.A., McCall R., Ferreira Ó., 2016. Predicting
672 coastal hazards for sandy coasts with a Bayesian Network. *Coastal Engineering*. 118, 21-34.

673 Rodrigues B.A., Matias A., Ferreira Ó., 2012. Overwash hazard assessment *Geologica Acta*. 10, 427-437.

674 Roelvink D., Reniers A., van Dongeren A., van Thiel de Vries J., McCall R., Lescinski J., 2009. Modelling
675 storm impacts on beaches, dunes and barrier islands. *Coastal Engineering*. 56, 1133-1152.

676 Santos F.D., Lopes A.M., Moniz G., Ramos L., Taborda, R., 2017. Grupo de Trabalho do Litoral: Gestão
677 da Zona Costeira: O desafio da mudança. Filipe Duarte Santos G.P.-L.e.A.M.L.E., Taborda R.,
678 2017. Grupo de Trabalho do Litoral: Gestão da Zona Costeira: O desafio da mudança. Lisbon.

679 Stelljes N., Martinez G., McGlade K., 2018. Introduction to the RISC-KIT web based management guide
680 for DRR in European coastal zones. *Coastal Engineering*. 134, 73-80.

681 Stronkhorst J., Huisman B., Giardino A., Santinelli G., Santos F.D., 2018. Sand nourishment strategies
682 to mitigate coastal erosion and sea level rise at the coasts of Holland (The Netherlands) and
683 Aveiro (Portugal) in the 21st century. *Ocean & Coastal Management*. 156, 266-276.

684 Sutherland J., Peet A., Soulsby R., 2004. Evaluating the performance of morphological models. *Coastal*
685 *Engineering*. 51, 917–939.

686 van Dongeren A., Ciavola P., Martinez G., Viavattene C., Bogaard T., Ferreira O., et al., 2018.
687 Introduction to RISC-KIT: Resilience-increasing strategies for coasts. *Coastal Engineering*. 134,
688 2-9.

689 van Dongeren A., Ciavola P., Martinez G., Viavattene C., DeKleermaeker S., Ferreira O., et al., 2016.
690 RISC-KIT: Resilience-increasing Strategies for Coasts. *E3S Web Conf.* 7, 17001.

691 Villatoro M., Silva R., Méndez F.J., Zanuttigh B., Pan S., Trifonova E., et al., 2014. An approach to assess
692 flooding and erosion risk for open beaches in a changing climate. *Coastal Engineering*. 87, 50-
693 76.

694 Vitousek S., Barnard P.L., Fletcher C.H., Frazer N., Erikson L., Storlazzi C.D., 2017. Doubling of coastal
695 flooding frequency within decades due to sea-level rise. *Scientific Reports*. 7, 1399.

696 Voudoukas M.I., Almeida L.P.M., Ferreira Ó., 2012a. Beach erosion and recovery during consecutive
697 storms at a steep-sloping, meso-tidal beach. *Earth Surface Processes and Landforms*. 37, 583-
698 593.

699 Voudoukas M.I., Ferreira O., Almeida L.P., Pacheco, A., 2012b. Toward reliable storm-hazard
700 forecasts: XBeach calibration and its potential application in an operational early-warning
701 system. *Ocean Dynamics*. 62, 1001-1015.

702 Voudoukas M.I., Mentaschi L., Voukouvalas E., Verlaan M., Feyen L., 2017. Extreme sea levels on the
703 rise along Europe's coasts. *Earth's Future*. 5, 304-323.

704 Voudoukas M.I., Mentaschi L., Voukouvalas E., Verlaan M., Jevrejeva S., Jackson L.P., et al., 2018a.
705 Global probabilistic projections of extreme sea levels show intensification of coastal flood
706 hazard. *Nature Communications*. 9, 2360.

707 Voudoukas M.I., Mentaschi L., Voukouvalas E., Bianchi A., Dottori F., Feyen L., 2018b. Climatic and
708 socioeconomic controls of future coastal flood risk in Europe. *Nature Climate Change*. 8, 776–
709 780.

710 Wright L.D., Short A.D., 1984. Morphodynamic variability of surf zones and beaches: a synthesis.
711 *Marine Geology*. 56, 93-118.

712 Wu W., Yan S., Feng R., Song D., Chen X., 2017. Development of an environmental performance
713 indicator framework to evaluate management effectiveness for Jiaozhou Bay Coastal Wetland
714 Special Marine Protected Area, Qingdao, China. *Ocean & Coastal Management*. 142, 71-89.

715 Ye G., Chou L.M., Yang S., Wu J., Liu P., Jin C., 2015. Is integrated coastal management an effective
716 framework for promoting coastal sustainability in China's coastal cities? *Marine Policy*. 56, 48-
717 55.

718 Zanuttigh B., Simcic D., Bagli S., Bozzeda F., Pietrantoni L., Zagonari F., et al., 2014. THESEUS decision
719 support system for coastal risk management. *Coastal Engineering*. 87, 218-239.

720